High-precision measurement of europium isotopic composition of geological reference materials by multi-collector inductively coupled plasma mass spectrometry (MC-ICP-MS)

Lukas Nicol, Marion Garçon, Maud Boyet, Abdelmouhcine Gannoun

JAAS

High-precision measurement of Europium isotopic composition of geological reference materials by Multi Collector Inductively Coupled Plasma Mass Spectrometry (MC-ICP-MS)

Journal:	*Journal of Analytical Atomic Spectrometry*
Manuscript ID	JA-ART-02-2023-000042.R2
Article Type:	Paper
Date Submitted by the Author:	04-Apr-2023
Complete List of Authors:	Nicol, Lukas; Université Clermont Auvergne, Laboratoire Magmas et Volcans Garçon, Marion; Université Clermont Auvergne, Laboratoire Magmas et Volcans Boyet, Maud; Université Clermont Auvergne, Laboratoire Magmas et Volcans GANNOUN, Abdelmouhcine; Université Clermont Auvergne, Laboratoire Magmas et Volcans

Submitted to Journal of Analytical Atomic Spectrometry

High-precision measurement of Europium isotopic composition of geological reference materials by Multi Collector Inductively Coupled Plasma Mass Spectrometry (MC-ICP-MS)

Lukas Nicol[1], Marion Garçon[1], Maud Boyet[1], Abdelmouhcine Gannoun[1]

[1] Université Clermont Auvergne, CNRS, IRD, OPGC, Laboratoire Magmas et Volcans, F-63000 Clermont-Ferrand, France

ABSTRACT

To date only few analyses of Europium (Eu) isotopic composition of terrestrial and extraterrestrial samples have been reported in the literature. This isotopic systematic remains largely understudied and it is still unknown whether the Eu isotopic composition of the Earth's major reservoirs show measurable variations. Here we present a comprehensive chemical protocol to separate Eu from different sample matrices and a method for measuring high-precision Eu isotopic composition by multi-collector inductively coupled plasma mass spectrometry (MC-ICP-MS). We show that the chemical separation of Eu by ion chromatography may induce measurable isotopic fractionation and that careful attention must be taken to limit analytical artefacts. As Eu has only two stable isotopes, we investigated different methods to correct as best as possible for instrumental mass bias. We found that doping the samples with Samarium (Sm), a close neighbor of Eu, provided the best precision and trueness. Based on complete duplicate analyses, we evaluated the repeatability standard deviation (2SD) of the whole procedure at about 50 ppm on the $^{151}Eu/^{153}Eu$ ratio (i.e. 0.5 ε unit), which is two to four times better than previously published procedures. All igneous and sedimentary reference materials analyzed in this study have Eu isotopic compositions similar to the reference standard NIST 3117a within uncertainties (i.e. $\varepsilon_{Eu} = 0 \pm 0.5$).

Keywords: Europium isotopes, MC-ICP-MS, NIST 3117a, Rare Earth Element

1 INTRODUCTION

Europium (Eu) is a rare-earth element (REE) with the atomic number 63. It is one of the most reactive REE as its reaction with oxygen rapidly forms oxides and it is sensitive to redox-conditions. Europium switches his valence from 3^+ to 2^+ depending strongly on (i) temperature and slightly on (ii) pH and (iii) pressure[1–5]. Natural Eu has two stable isotopes: ^{151}Eu and ^{153}Eu with respective abundances of 47.81 % and 52.19 %, (^{153}Eu/^{151}Eu = 1.0916 ± 0.0034)[6]. Due to the absence of a third stable isotope, the correction of instrumental mass bias to determine high-precision Eu isotopic ratios is quite challenging. In this study, we tested several methods (sample-standard bracketing, doping with different neighbor elements) to determine the best way to precisely measure the Eu isotopic composition of geological samples.

So far, only a few studies have reported Eu isotopic composition of terrestrial and extraterrestrial samples[7–9]. All studies have used MC-ICP-MS techniques. Arantes De Carvalho et al.[7] investigated the isotopic composition of five samples of natural water, with a repeatability of ±1.4 ε (2SD estimated from the repeated measurement of their Eu standard solution from Merck (Darmstadt, Germany)), and measured no significant variation in their samples. Moynier et al.[8] analyzed three terrestrial samples (one basalt and two soils), three chondrites and six separated chondrules, with a repeatability of ± 2 ε (2SD estimated from the repeated measurement of their Eu standard solution JMC) and found that the Eu isotopic composition of three calcium-aluminum inclusions from Allende chondrite were different from other terrestrial and extra-terrestrial samples (-11.8, -11 and -7.8 ε). They interpreted this mass fractionation as being due to preferential evaporation of ^{153}Eu during very early solar system processes. Lee and Tanaka[9,10] analyzed six high-purity Eu reagents, nine geological reference standards with igneous matrices and ten Korean granites with various magnitudes of Eu anomalies. These authors[10] presented a detailed chemical protocol to separate Eu and showed that purification processes fractionate the ^{153}Eu/^{151}Eu ratio with high ^{153}Eu/^{151}Eu ratios at the beginning of the elution peak to low ratios at the end of the elution peak. In addition, they showed that industrial processes affect the Eu isotopic composition of reference materials. We estimated their repeatability at about ± 1.6 ε (2SD) based on complete duplicate analyses. Most of the geological rock standards analyzed by Lee and Tanaka[10,11] show no Eu isotopic fractionation within their uncertainties but they suggested that felsic igneous rocks with high SiO_2 content (> 75 wt.%) and notable negative Eu anomaly (0.1

to 10 times lower than the chondritic composition) have a lighter Eu isotopic composition than the reference standard (Eu NIST 3117a)[9]. This variability is interpreted to be linked to Ca-feldspar crystallization and more widely to magmatic differentiation processes. Further investigations of the variability of Eu isotopes in igneous rocks and in Earth's major reservoirs in general are needed to confirm this fractionation trend.

In this study, we present a new chemical protocol to isolate Eu from different geological matrices. We investigated key factors that influence the precision and trueness of Eu isotopic analyses: (i) the isotopic fractionation during column chemistry, (ii) the effect of Ba oxides during MC-ICP-MS measurements and (iii) the instrumental mass bias correction. Finally, we report reference values for the NIST 3117a standards and 10 geological reference materials (igneous and sediment samples) with a better repeatability than previous studies.

2 ANALYZED REFERENCE MATERIALS

Chemical separations and isotopic measurements were performed on both (i) synthetic reference materials and (ii) geological reference materials of variable compositions. We used the reference material NIST 3117a for Eu (Lot No. 120705), NIST 3147a for Sm (Lot No. 140115) and NIST 3118a for Gadolinium (Gd, Lot No. 992004) for testing different schemes of instrumental mass bias correction. Ten igneous and sedimentary reference materials have been also analyzed. Nine igneous rocks were selected to cover a large range of chemical compositions: two andesites (AG-V 1, AG-V 2), one anorthosite (AN-G), three basalts (BCR-1, BHVO-2, BIR 1a), one granite (G-2) and one rhyolite (RG-M). The two terrigenous sediments are JLk-1 and JSd-2.

3 CHEMISTRY

3.1 Sample digestion

Approximatively 100 mg of fine powdered rocks (igneous rocks and sediments) were digested using two different techniques. The first one is a modified version of the method

published by Yu et al.[12] consisted in adding a mixture of concentrated HF (29 M) and HNO_3 (14 M) in a ratio 3:1 (usually 3 mL of HF for 100 mg of powdered rocks) in 15 mL PFA Savillex® beakers. Hydrofluoric acid (HF) should be handled with great care, using cleaned chemically resistant butyl gloves and safety goggles, under a hood. The closed beakers were left on a hot plate at 110 °C for 72h and then evaporated to dryness. The second technique consisted in adding double distilled NH_4HF_2 in the sample powder (400 mg for 100 mg of powdered rock) in a closed 15 mL PFA Savillex® beakers at 230 °C for 24 h in an electric oven. The beakers were closed by hand, not too tight to avoid over-pressure. The atmosphere in the oven was continuously exhausted. This technique is more efficient than regular HF to digest refractory grains such as zircons[13]. The digestion technique used for each of the analyzed geological reference materials is indicated in Table 3. After the first step of digestion, the samples were successively treated at 110°C with 5 mL of concentrated HNO_3 (14 M), 5 mL HCl (12N) and *aqua regia* (HCl-HNO_3 mixture in a molar ratio of 3:1) made with 4 mL of concentrated HCl (12 M) and 1.14 mL of concentrated HNO_3 (14 M).

3.2 Chemical separation of Eu

To obtain a near-perfect separation of Eu from the sample matrix we developed a three-step chemical procedure (Table 1). First, REEs were isolated from the matrix using 2 mL of cation exchange resin AG®50W-X8 (200-400 mesh) in a Biorad™ column (c.f. Figure 1A for column dimensions). Samples were loaded in 2.5 M HCl after centrifugation, major elements were discarded with 2.5 M HCl and REEs were collected in 6 M HCl. Then the REE fractions were purified from Ba with 250 μL of Eichrom™ TRU resin (50-100 μm), in a quartz glass column, because BaO masses interfere on Eu masses during MC-ICP-MS measurements (c.f. section 5.3). Samples were loaded in 1 M HNO_3 and Ba was separated from REEs with 1 M HNO_3. Finally, REEs were collected with 0.05 M HNO_3. The last step of the separation protocol was done with a quartz glass column of 400 mg of Eichrom™ LN resin (20-50 μm) in 0.5 M HCl. With this column we collected Eu without any detectable amount of Sm or Gd (see Figure 1B). As a result Eu was isolated from other elements and we minimized matrix effect as much as possible (e.g.[14,15]).

This method has the advantage to avoid the use of organic acid such as the 2-hydroxyisobutyric acid (HIBA) used by Lee and Tanaka[10] in their Eu separation protocol since the presence of residual organic compounds may interfere on the isotopic measurement[16].

After the chemistry, the amount of Eu and the purity of the collected Eu fractions were systematically monitored by analyzing a small aliquot of the samples (around 3 % taken from the samples diluted in 2 mL of nitric solution) on an Agilent 7500 Q-ICP-MS (Agilent Technologies™) at the Laboratoire Magmas & Volcans (LMV) in Clermont-Ferrand (France). For each batch of ten samples, we processed a NIST standard to ensure complete recovery of Eu and the absence of isotopic fractionation induced by column chemistry. Yields were calculated using a calibration curve made from a synthetic solution (CMS solutions containing more than 60 trace elements in different concentrations from 0.01 ppb to 100 ppb). Recovery yields measured on processed NIST standards were always higher than 90 % (Table 2). For geological reference materials, the yields ranged between 79 to 100% (Table 3). Finally, the amount of Ba in the separated Eu fractions was thoroughly controlled to make sure their Ba/Eu ratios did not exceed 0.07 (c.f. section 5.3). Total procedural blanks, including digestion and processing through column chemistry, were always lower than 0.1 ng of Eu (42 pg, 60 pg, 100 pg, 15 pg, 44 pg, 10 pg; n = 6) whatever the digestion method. Such amounts are considered negligible relative to the amount of Eu present in the samples (usually 50 – 100 ng).

4 MASS SPECTROMETRY FOR EU ISOTOPIC MEASUREMENTS

Isotopic measurements were performed on the LMV Neptune Plus MC-ICP-MS (ThermoFisher Scientific™). The sample were introduced into the instrument using an Aridus II desolvator (CETAC Technologies™) which increases the sensitivity of the signal and reduces the oxidation rate (c.f. Table 4 for detailed instrument settings). The nine Faraday cup configuration was set up to measure Eu, Sm and Gd isotopes (Table 5). We typically analyzed solutions concentrated at 10-20 ppb of Eu in 0.05 M HNO_3 to reach a sensitivity of about 9 - 10 V on ^{151}Eu using a 100 µL/min nebulizer.

Because Eu has only two isotopes, we tested several methods to correct for instrumental mass fractionation: (i) external normalization using the sample-standard bracketing technique, (ii) internal normalization using either the Sm NIST 3147a

standard or the Gd NIST 3118a standard added to the sample. Adding a different element to the sample for correcting instrumental mass bias has been developed for Cu and Zn isotopic analyses by Marechal et al.[17]. We decided to compare results obtained using two neighboring elements of Eu: Sm and Gd because they have several stable isotopes with masses near to those of Eu.

As the oxide formation impacts isotopic measurements (e.g.[18]), the oxidation rates of Eu, Sm and Gd were systematically controlled before each sequence of measurement (twice a day) so that it never exceeded 0.01% for Eu oxides (i.e. EuO/Eu ratio) and 0.15 % for both Sm and Gd oxides. If necessary, the oxidation rates were optimized mainly by adjusting the torch position. The formation of hydroxides was also controlled but was found always negligible compared to oxide formation.

A typical sequence of measurement consisted in analyzing about seven Eu NIST 3117a to check for instrument stability and repeatability, then samples were measured in between NIST standards to calculate epsilon values. Previous studies[7,9] reported delta values (per mil) relative to the Eu NIST 3117a. In this study, we prefer to report epsilon values (per 10 000) as it better expresses the natural range of variations measured in geological materials so far. Thereafter, we will use the following notation:

$$\varepsilon_{Eu} = \left(\frac{(^{153}Eu/^{151}Eu)_{\text{ sample}}}{(^{153}Eu/^{151}Eu)_{\text{ NIST standard}}} - 1 \right) * 10^4 \qquad \text{(Eq. 1)}$$

5 RESULT AND DISCUSSION

5.1 Instrumental mass bias correction

5.1.1 Sample-standard bracketing vs. Element doping with Gd and Sm

In this section, we evaluated which instrumental mass bias correction was the most appropriate to measure high-precision Eu isotopic compositions. We compared the sample-standard bracketing method to element doping (Sm and Gd) on the same sequences consisting of repeated measurements of Eu NIST 3117a standards that have

been doped with Sm or Gd (Figure 2 and Appendix - Table 1). Data reduction was calculated offline.

The first method we tested was the sample standard bracketing technique[19] that consists in calculating an average fractionation factor β using the previous and following NIST standards in the measurement sequence. We calculated mass fractionation-corrected ratios using the exponential law, which is the most accepted law to correct for instrumental mass bias during MC-ICP-MS measurements[19,20] following equation (2):

$$\left(\frac{^{153}Eu}{^{151}Eu}\right)_{FC,\ sample} = \left(\frac{^{153}Eu}{^{151}Eu}\right)_{Meas,\ sample} * \left(\frac{m^{153}Eu}{m^{151}Eu}\right)^{\left(\frac{\beta_{Eu\ Previous\ std} + \beta_{Eu\ Following\ std}}{2}\right)} \quad \text{(Eq. 2)}$$

$$\beta_{Eu,\ std} = \frac{\ln\left(\frac{\left(\frac{^{153}Eu}{^{151}Eu}\right)_{True}}{\left(\frac{^{153}Eu}{^{151}Eu}\right)_{Meas,\ std}}\right)}{\ln\left(\frac{m^{153}Eu}{m^{151}Eu}\right)} \quad \text{(Eq. 3)}$$

"FC" stands for fractionation corrected ratio, "Meas" stands measured ratios and m are the masses of the isotopes in amu. Here we used the masses given by Audi et al.[21]. "True" corresponds to the reference value adopted for the $^{153}Eu/^{151}Eu$ ratio. Here we used $(^{153}Eu/^{151}Eu)True = 1.0916$ following Meija et al.[6].

From the Eu fractionation-corrected ratio, we calculated ε_{Eu} as described in equation (4):

$$\varepsilon_{Eu} = \left(\frac{(^{153}Eu/^{151}Eu)_{FC,\ sample}}{\left(\left(\frac{^{153}Eu}{^{151}Eu}\right)_{FC,\ previous\ NIST} + \left(\frac{^{153}Eu}{^{151}Eu}\right)_{FC,\ following\ NIST}\right)/2} - 1\right) * 10^4 \quad \text{(Eq. 4)}$$

in which "FC" stands for fractionation corrected, "previous NIST" and "following NIST" corresponds to unprocessed NIST 3117a measured just before and after the sample in the MC-ICP-MS measurement sequence. Results obtained by this method on NIST standards are shown in Figure 2.

The second method (element doping) consists in adding an element in the separated Eu solution just before the measurement; the aim being to use this element to monitor and correct for instrumental mass fractionation. The advantage of using the element doping technique over sample-standard bracketing is that the mass fractionation correction reflects the faith of isotopes at the time of the measurement while sample-standard bracketing interpolates the fractionation trend between standards over time. The inconvenient however is that elements do not all fractionate the same way in the instrument. Doping elements will never perfectly capture the fractionation behavior of Eu but can provide a good approximation of it. Here, we tested the addition of Sm and Gd because they are neighboring elements of Eu in the periodic table, hence they have more chances to behave similarly regarding mass fractionation during MC-ICP-MS measurements. We initially added twice more Sm (or Gd) than Eu to get enough signal to properly calculate the mass fractionation factors β. In Section 5.2, we evaluated the effects of doping the Eu solutions with variable Eu/Sm ratios on the precision and trueness of Eu isotopic analyses. At first, we simply assumed that the fractionation factors of Sm and Gd were strictly similar to the fractionation factor of Eu so that $\beta_{Eu} = \beta_{Sm}$ or $\beta_{Eu} = \beta_{Gd}$. As for the sample-sample bracketing method, we used the exponential law to correct for mass instrumental fractionation following equations (5) and (7):

Using Sm as a dopant:

$$\left(\frac{^{153}Eu}{^{151}Eu}\right)_{FC} = \left(\frac{^{153}Eu}{^{151}Eu}\right)_{Meas} * \left(\frac{m^{153}Eu}{m^{151}Eu}\right)^{\beta_{Sm}} \qquad (Eq.\ 5)$$

$$\text{with } \beta_{Sm} = \frac{\ln\left(\frac{\left(\frac{^{149}Sm}{^{147}Sm}\right)_{True}}{\left(\frac{^{149}Sm}{^{147}Sm}\right)_{Meas}}\right)}{\ln\left(\frac{m^{149}Sm}{m^{147}Sm}\right)} \qquad (Eq.\ 6)$$

Using Gd as a dopant:

$$\left(\frac{^{153}Eu}{^{151}Eu}\right)_{FC} = \left(\frac{^{153}Eu}{^{151}Eu}\right)_{Meas} * \left(\frac{m^{153}Eu}{m^{151}Eu}\right)^{\beta_{Gd}} \qquad (Eq.\ 7)$$

$$\text{with } \beta_{Gd} = \frac{\ln\left(\frac{\left(\frac{^{157}Gd}{^{155}Gd}\right)_{True}}{\left(\frac{^{157}Gd}{^{155}Gd}\right)_{Meas}}\right)}{\ln\left(\frac{m^{157}Gd}{m^{155}Gd}\right)} \qquad (Eq.\ 8)$$

where "FC" stands for fractionation corrected ratio, "Meas" for measured ratios and m are the masses of the isotopes in amu.

We used $(^{149}\mathrm{Sm}/^{147}\mathrm{Sm})_{\mathrm{True}} = 0.9216$[22–25] when samples were doped with Sm and $(^{157}\mathrm{Gd}/^{155}\mathrm{Gd})_{\mathrm{True}} = 1.0576$[23,25–27] when samples were doped with Gd. After the chemistry, our Eu fractions contain no detectable Sm (below the detection limit of the Q-ICP-MS) but can have some Gd (usually < 0.5 % of the total Gd). This has however no consequence on the measured Gd isotopic composition because an enough large quantity of Gd is added by doping. Figure 2 represents typical measurement sequences and clearly shows that the element doping technique, whether Sm or Gd are used, improves the repeatability of the same sequence. Typical repeatability (2SD) for the sample-standard method is in the order of 1 ε while element doping allows us to reach repeatability (2SD) down to 0.3 ε. The mean repeatability standard deviation for the Eu-Sm couple is around 0.38 ε (2SD, n

$= 10$) against 0.60 ε (2SD, $n = 12$) for the Eu-Gd couple. Coupling Eu with Sm thus appears to be the best method for correcting instrumental mass fractionation. We note that the ionization energy of Sm is closer to that of Eu than that of Gd[28]. This might be the reason why the fractionation behavior of Sm is more appropriate to correct for Eu instrumental mass bias. Thereafter, we will use this method to determine Eu isotopic compositions in synthetic and geological reference materials.

5.1.2 Relationship between β_{Sm} and β_{Eu}

Once we have chosen Sm for correcting instrumental mass bias, we explored the relationship between β_{Eu} and β_{Sm} to see whether our first approximation assuming that $\beta_{Eu} = \beta_{Sm}$ could be improved. Figure 3.A shows β_{Eu} and β_{Sm} values calculated for Eu NIST 3117a standards in three different measurement sequences.

As previously highlighted for Copper (Cu) and Zinc (Zn)[17], the logarithms of $^{65}Cu/^{63}Cu$ and $^{68}Zn/^{64}Zn$ ratios are linearly correlated, implying a close fractionation behavior of the two elements during MC-ICP-MS measurements. Here, we explored the relationship between β_{Eu} and β_{Sm}, which correspond to the logarithms of $^{153}Eu/^{151}Eu$ and $^{149}Sm/^{147}Sm$ ratios divided by constants (c.f. equations 3 and 6). We found that β_{Eu} was linearly correlated with β_{Sm} in each of the three sequences (Figure 3A; $R^2 > 0.9$). The linear trend is also observed when plotting the logarithms of $^{153}Eu/^{151}Eu$ and $^{149}Sm/^{147}Sm$ ratios but is not shown here. We determined the equations of the linear trends for each individual sequence using a weighted linear regression as implemented by York et al.[29] so that:

$$\beta_{Sm} = a \times \beta_{Eu} + b \qquad \text{(Eq. 9)}$$

in which "a" stands for the slope and "b" for the intercept.

The slopes of the regressions are always close to 1 (average value $= 0.99 \pm 0.14$, 2SD) but the intercepts can significantly differ from one sequence to another (i.e. from 0.07 to 0.44) (Figure 3.A and Table 6). Using the regression line of each sequence and the measured β_{Sm}, we can estimate a $\beta_{Eu\ corrected}$ for each sample and inject this value in the following equation (Eq. 10) to correct for instrumental mass fractionation.

$$\left(\frac{^{153}Eu}{^{151}Eu}\right)_{FC} = \left(\frac{^{153}Eu}{^{151}Eu}\right)_{Meas} * \left(\frac{m^{153}Eu}{m^{151}Eu}\right)^{\beta Eu\ corrected} \qquad (Eq.\ 10)$$

where "FC" stands for fractionation corrected ratio, "Meas" for measured ratios and m are the masses of the isotopes in amu.

Figure 3.B compares the effects of the two corrections ($\beta_{Eu} = \beta_{Sm}$ and $\beta_{Eu\ corrected}$ estimated from the weighted regression line) on the Eu isotopic compositions of Eu NIST 3117a analyses. In most cases, the use of the regression line improved both the trueness and the precision of the measurements. The average Eu isotopic composition of NIST 3117a corrected with $\beta_{Eu\ corrected}$ is closer to zero than those corrected with β_{Sm} and the precision is improved by a few ppm (between 5 and 10 ppm). Thereafter, we thus systematically determined the equation of the regression line between β_{Sm} and β_{Eu} using the measured isotopic compositions of all Eu NIST 3117a standards run during the measurement sequence. Then we used this regression line to calculate $\beta_{Eu\ corrected}$ from the measured β_{Sm} in each analyzed sample. This calculation was done offline, once the sequence is over, to ameliorate the instrumental mass bias correction and reach the best possible repeatability on Eu isotopic ratios.

5.2 Effect of variable Eu/Sm ratios on the quality of Eu isotopic analyses

To test whether variable Eu/Sm ratios in the analyzed solutions had an effect on the precision and/or trueness of Eu isotopic measurements, we measured several series of Eu NIST 3117a standards doped with variable amounts of Sm NIST 3147a during three different measurement sequences (Figure 4 and Appendix Table 3). This test is crucial since the Eu/Sm ratios of the analyzed solutions can vary (i) from one sample to another, (ii) between sample and standard, (iii) through the measurement sequence, (iv) from one sequence to another. This is because the amount of Eu present in the samples may not be known precisely, for example if yields are not properly estimated before isotopic analyses, and because Sm and Eu are not ionized the same way through the sequence or from one sequence to another. Hopefully, our results demonstrated that Eu isotopic compositions are not very sensitive to the Eu/Sm ratios in the analyzed NIST standards (Figure 4). We

obtained similar ε_{Eu} values for a large range of $^{151}Eu/^{147}Sm$ ratios with an average value of -0.1 $\pm$ 0.60 (2SD, n = 66) when all data are considered and an average value of 0 $\pm$ 0.52 (2SD, n = 56) if we only consider $^{151}Eu/^{147}Sm$ ratios between 0.2 and 5. No significant trend is observed as a function of $^{151}Eu/^{147}Sm$ ratios when $^{151}Eu/^{147}Sm$ ratios are below 5. There might be a trend towards negative values for $^{151}Eu/^{147}Sm$ ratios > 5 but further analyses are required to confirm this hypothesis. We did not perform additional tests because analyses having $^{151}Eu/^{147}Sm$ ratios > 5 are an extreme scenario that we never encountered in our study. It also implies that Sm would be measured at too low signals to obtain high enough precision on beta values.

Our Eu isotopic analyses were all performed within a range of $^{151}Eu/^{147}Sm$ ratios between 1.5 and 3 for both standards and samples. To have a better control on the range of $^{151}Eu/^{147}Sm$, we systematically analyzed an aliquot of the separated Eu fraction out of the separation procedure (usually 3%) by Q-ICP-MS before the isotopic analyses on MC-ICP-MS. This allowed us to precisely determine the amount of Eu present in the sample and thus adjust the amount of Sm that needed to be added to make sure $^{151}Eu/^{147}Sm$ ratios did not spread over a large range of values.

5.3 Effect of Ba oxides on the measurement of Eu isotopic compositions

Europium isotopes (^{151}Eu and ^{153}Eu) have no direct isobaric interferences with other elements from the periodic table but Ba oxides under the forms $^{135}Ba^{16}O$ and $^{137}Ba^{16}O$ are potential interferants on masses 151 and 153. Barium is relatively difficult to separate from REEs using ion chromatography and its concentration is usually one to three orders of magnitude higher than Eu in geological samples. In this section, we tested whether the presence of residual Ba after chemical separation and the formation of Ba oxides during MC-ICP-MS measurements could alter the quality of Eu isotopic measurements. Moynier et al.[8] used a theoretical mixing curve between a solution of Eu and Sm and another one made of Eu, Sm, and BaO to prove the non-influence of Ba on their Eu isotopic measurements. Here we measured a solution containing the same amount of Eu (NIST 3117a) and Sm (NIST 3147a) but variable amounts of Ba (mono-elemental solution from Sigma-Aldrich®) to evaluate the influence of the presence of BaO during Eu isotopic measurements (yellow data points on Figure 5). We controlled the oxidation rate of Ba

before and after the sequence and estimated that 0.8 % of Ba was converted into BaO. We compare these results to a theoretical model that predicts the deviation of ε_{Eu} as a function Eu/Ba ratio for different oxidation rates. Our measurements perfectly follow the predicted model with a range of ε_{Eu} from + 0.5 (Ba/Eu = 0.1) to + 16 (Ba/Eu = 3), showing that the presence of Ba oxides significantly degrade the quality of Eu isotopic measurements.

Both the measurements and the theoretical model show that Eu isotopic compositions are very sensitive to the amount of residual Ba in the samples when the oxidation rate exceeds 0.1%. If the oxidation rate of Ba is around 1%, as during the measurement sequence shown in yellow in Figure 5, Eu isotopic compositions can be biased by several epsilon as soon as the Ba content exceeds one third of the Eu content in the measured fraction. In general, we thus recommend that the Ba content be checked by Q-ICP-MS in each sample before analysis. The maximum Ba/Eu ratio should be 0.07 to guarantee a repeatability of 0.5 ε (2SD) on Eu isotopic compositions (c.f. section 5.5).

5.4 Isotopic fractionation during column chemistry

Lee and Tanaka[10] were the first to report a detailed methodology to isolate Eu from geological sample matrices. Their chemical procedure differs from the one described here as they used a cation-exchange resin (Biorad AG® 50WX-8 200–400mesh) column with 2-hydroxyisobutyric acid (0.12 M HIBA) as eluent to separate Eu from other REEs. They showed that processing the samples through this column fractionates Eu isotopes and leads to, respectively, heavier and lighter Eu isotopic compositions in the front and tail of the Eu elution peak. With this acid, heavy REEs are eluted before light REEs. Comparable isotopic fractionations were observed for Nd using similar column chromatography experiment[30]. Our last column is different from that of Lee and Tanaka[10] and involves LN resin and HCl as eluent (Figure 1). Because previous studies (e.g.[31]) have reported Nd isotopic fractionation for samples processed through LN resin, we tested whether this final purification step could be partly responsible for the variability measured in Eu NIST 3117a standards processed through all columns.

We first loaded 1000 ng of Eu NIST 3117a on two different LN-spec columns and collected the Eu elution peak in 10 different fractions on each column. We measured both

the amount of Eu (and obtained a yield relative to the total quantity loaded) and the Eu isotopic compositions of each collected fraction (Appendix - Table 5). The results demonstrate that $^{153}Eu/^{151}Eu$ ratios are strongly fractionated during elution with positive ε_{Eu} shifts (heavier isotopic compositions) in the first fractions up to $\varepsilon_{Eu} = +9.2$ and negative values (lighter isotopic compositions) at the tail of the elution peak up down to -3.0 (Figure 6A). Though the isotopic fractionation induced by processing the samples through the LN resin might appear significant, this must be weighted by the low amount of Eu present in the front and tail fractions (at best a few %). This is what is shown in Figure 6.B where we calculated the ε_{Eu} of the cumulated collected fractions as a function of the cumulated yield. The two trends represent the cumulated isotopic composition starting from the front to the tail of the peak and from the tail to the front of the peak (see caption for more details). For the two tested columns, we ended up having a cumulated ε_{Eu} of +0.6 and +0.1 when 99% and 94% of Eu were respectively collected. Note that the discrepancy between the cumulated ε_{Eu} and the yields may simply reflect the imprecision on the calculated yield. We took an aliquot of only 3% of the total collected fraction in a 2mL solution to measure the Eu yields on Q-ICP-MS. The low weight of the aliquot strongly limits the precision on the yields which could be at ± 10%. The two curves represented in Figure 6.B show that missing the front and/or the tail of the peak when collecting the Eu fraction on the LN column can fractionate Eu isotopic composition. This means that the Eu yield should be as high as possible to guarantee a repeatability of ± 0.5 epsilon units.

Finally, we processed a series of Eu NIST 3117a standards (N = 9; 100 ng of Eu each) through the LN fraction and collected the whole elution peak in one fraction for each of them. We measured the Eu yields on Q-ICP-MS and their Eu isotopic compositions on MC-ICP-MS. Results are listed in Table 2 and show very limited isotopic fractionation at the exit of the LN column. ε_{Eu} span a restricted range of values from -0.1 to +0.4 with yields always higher than 90 %. To evaluate the amplitude of potential isotopic fractionation during chemical separation, we always processed the Eu NIST 3117a standard through all columns with samples. The Eu isotopic composition of the NIST 3117a processed through chemistry together with the reference materials are reported in Table 2. The resulting ε_{Eu} values range between -0.5 to -0.2 and the Eu yields are all > 97 %.

5.5 Estimated repeatability for the measurement of Eu isotopic compositions

To evaluate the repeatability of Eu isotopic analyses, we first considered at the average isotopic composition of Eu NIST 3117a standards for each sequence of measurements over about one year of analyses (Table 6 and Figure 7). These measurements were performed by doping with Sm to correct for instrumental mass fractionation and with the best possible instrumental conditions (low oxide formation rate, high sensitivity). Taking into account the analyses of NIST 3117a standards only yields an average precision (2SD) of 0.29 ε for the 26 measurement sequences. Given the isotopic fractionation produced by the processing of samples through column chemistry if the entire elution peak is not collected, especially on the LN resin (c.f. section 5.4), we estimated the repeatability of Eu isotopic compositions at ± 0.5 ε (2SD). Our method therefore provides a precision two to four times better than previous studies, which makes it possible to detect smaller Eu isotopic variations within natural samples.

6 EU ISOTOPIC COMPOSITIONS OF GEOLOGICAL REFERENCE MATERIALS

Results obtained for various geological reference materials including igneous rocks ranging from basalts to granites, as well as terrigenous sediments, are presented in Table 3. Few reference materials were digested following different techniques (HNO_3-HF and NH_4HF_2 c.f. section 3.1). For most samples, rerun (same separated fraction analyzed several times) and duplicates (different dissolution of the same sample) were analyzed. Reruns give always similar Eu isotopic composition within uncertainties.

We note that the 2SE associated with the NH_4HF_2 digestion is systematically higher than those obtained with HF-HNO_3 digestion. The 2SD calculated from NIST standards measured during the sequence of the NH_4HF_2 digestion duplicates is higher than other 2SD (2SD = 0.42, n = 13) and could explain those variations. Furthermore, yields are different between HF-HNO_3 and NH_4HF_2 digested-samples. In general, yields values are difficult to interpret because they do not correlate with ε_{Eu} values, in particular low yields are not systematically associated to fractionated ε_{Eu} values. Two main reasons can explain

the absence of correlation. First, we estimate the precision of the yields to be at ± 10% since we do not precisely weight the aliquots and solutions before analyses on Q-ICP-MS. With such a low precision, it may be difficult to see a proper correlation between yields and ε_{Eu} values. Secondly, small fractions of Eu can be lost at different steps of the chemistry without producing Eu isotopic fractionation (e.g. if some sample remains in the beaker when it is loaded on a column). The formation of fluorides could maybe impact the recovery yields of Eu[32] without fractionating it. However, we made sure to dissolve all fluorides through the digestion procedure. We systematically centrifuged the samples before loading onto the first cation exchange resin AG®50W-X8. If the presence of fluorides was suspected (i.e. presence of gel material or precipitate), the sample was set aside and retreated with concentrated HNO_3 at high temperature to dissolve the residual solids. However, if the entire Eu peak is not collected out of the last column (LN resin), the ε_{Eu} value can be shifted towards negative or positive values depending on whether the beginning or the tail of the peak is lost. To make sure all Eu has been collected during this crucial step of the purification process, we now collect the fractions before and after the Eu elution peak on the LN column and quantify the amount of Eu present in each collected fraction. That being said, the variations of ε_{Eu} between samples, reruns and duplicates are systematically within the range of the established 2SD at ± 0.5 ε, meaning that our procedure do not fractionate Eu isotopic compositions outside estimated uncertainties.

As shown in Figure 8, the Eu isotopic composition of the geological reference materials analyzed in this study is similar to the NIST 3117a considering the repeatability standard deviation at 2SD = ± 0.5 ε. So far, all measured geological reference materials, including variably differentiated igneous rocks and terrigenous sediments, have the same Eu isotopic composition as the NIST 3117a standards within uncertainties. Although our data span a large range of SiO_2 contents, we do not observe any variation of the ε_{Eu} as a function of magmatic differentiation as suggested by Lee and Tanaka[9]. However, we did not measure as much granites as they did, nor samples with very high SiO_2 content (i.e. > 75 wt.%) and cannot confirm the trend they suggest.

7 CONCLUSION

The results of our study show that measuring the Eu isotopic composition is challenging because Eu has only two isotopes. Obtaining a good precision is crucial because the expected isotopic variations in natural samples are rather small. We described a detailed three-step column chemistry protocol for isolating Eu from geological sample matrices. The last step involving LN resin is the most critical and requires the highest possible yields to limit analytical isotopic fractionation. We compared several methods of correction for instrumental mass fractionation during MC-ICP-MS measurements. Doping Eu fractions with Sm ($1.5 < {}^{151}Eu/{}^{147}Sm < 3$) and determining the linear relationship between β_{Eu} and β_{Sm} provided the best repeatability. We found that the principal isobaric interferences on Eu isotopes during MC-ICP-MS measurements were the formation of BaO oxides and recommend that Ba/Eu ratios be lower than 0.07 to guarantee the best possible trueness. Following all these recommendations, we estimated the repeatability (2SD) of the whole procedure to be at $\pm$ 0.5 on ε_{Eu} values. So far, all measured geological reference materials, including variably differentiated igneous rocks and terrigenous sediments, have the same Eu isotopic composition as the NIST 3117a standard within uncertainties.

Author contributions

L.N., M.G. and M.B. designed the study and the method to analyze Eu isotopic compositions. L.N. carried out the chemical separation. L.N. and A.G. performed the measurements on mass spectrometers. All authors discussed the results and commented on the manuscript at all stages.

Conflicts of interest

The authors declare no conflicts of interest.

Acknowledgements

This study was funded by the European Research Council (ERC Starting Grant – GOforISOBIF, Grant agreement N° 852239). This is contribution no. XXX of the ClerVolc program of the International Research Center for Disaster Sciences and Sustainable Development of the University of Clermont Auvergne. We thank Chantal Bosq (LMV, Clermont-Ferrand, France) for always giving her best to give us optimal working conditions in the clean laboratory, Jean-Luc Piro (LMV, Clermont-Ferrand, France) for always ensuring a free slot at the ICP-MS, Krzysztof Suchorski (LMV, Clermont-Ferrand, France) for his advices in the clean laboratory and Delphine Auclair (LMV, Clermont-Ferrand, France) for helpful discussions. We thank the editor for the efficient handling of the manuscript and the three anonymous reviewers that provided comments on this manuscript.

Tables

Table 1 Chemical protocol used for the purification of Eu using column chromatography techniques

Table 2 Isotopic composition of NIST 3117a processed through chemistry

Table 3 Eu isotopic composition of geological reference materials

Table 4 Neptune Plus MC-ICP-MS Instrument settings

Table 5 Cup configuration used to analyze Eu isotopic compositions on the Neptune Plus MC-ICP-MS

Table 6 Average Eu isotopic compositions of NIST 3117a standards

Figure captions

Figure 1 Three-step procedure to separate Eu from the sample matrix

A) Column geometry and resins used at each step of the protocol. The detailed protocol including the amounts and types of acids used is shown in Table 1.
B) Elution profile for Sm, Eu, and Gd on the LN-spec resin (third step of the protocol). The profile was obtained by loading a synthetic REE solution (3 µg of each REE), collecting the fractions every 0.5 mL, and measuring their REE contents by Q-ICP-MS.

Figure 2 Comparison between three different methods to correct for instrumental mass fractionation

Eu isotopic compositions of NIST 3117a corrected by sample-standard bracketing (blue points) and element doping assuming $\beta_{Sm} = \beta_{Eu}$ or $\beta_{Gd} = \beta_{Eu}$ (yellow points for Sm, red points for Gd). SD stands for standard deviation. N corresponds to the number of NIST 3117a standards measured during the sequence.

Figure 3 Relationship between β_{Sm} and β_{Eu} in NIST 3117a standards doped with NIST 3147a Sm

A) Weighted linear regression between β_{Sm} and β_{Eu} calculated in NIST 3117a standards doped with Sm during three different measurement sequences.
B) Comparison of the repeatability obtained on NIST 3117a standards assuming $\beta_{Sm} = \beta_{Eu}$ or $\beta_{Eu} = a \times \beta_{Sm} + b$ (weighted linear regression as shown in A) for the same measurement sequences as presented in A.

Figure 4 Influence of the $^{151}Eu/^{147}Sm$ ratio on the Eu isotopic composition of NIST 3117a standards doped with NIST 3147a Sm

Our estimated precision on ε_{Eu} is shown by the horizontal grey bands (+/- 0.5 **ε** units).

Figure 5 Ba oxide interferences on Eu isotopic composition

Yellow points correspond to the analyses of a series of NIST 3117a standards (Eu concentration = 10 ppb) doped with variable amount of Ba to generate Ba/Eu ratios between 0.1 and 3 (ratio expressed in concentration). Black and grey lines correspond to theoretical models that predict the Eu isotopic compositions of NIST 3117a standards as a function of the amount of Ba (i.e. Ba/Eu ratio) and the formation of Ba oxide in the instrument (i.e. 0.1%, 0.5%, 0.8%, 1%, 2% of BaO). From the analyses of pure Ba solutions of known concentrations on 2022/10/18, we estimated the theoretical contribution of $^{135}Ba^{16}O$ and $^{137}Ba^{16}O$ on masses 151 and 153 for different oxide formation rates. Then we added this contribution to the Eu signal measured on masses 151 and 153 for NIST 3117a standards (about 9V on mass 151 and 10V on mass 153) and corrected instrumental mass fractionation using the exponential law as detailed in section 5.1. Based on theoretical models and assuming a maximum Ba oxide rate of 1%, Ba/Eu ratios should not exceed 0.07 to guarantee a repeatability of ± 0.5 ε unit.

Figure 6 Fractionation of Eu isotopic compositions through the LN resin

A) Eu isotopic composition of NIST 3117a fractions collected every 0.5 mL during the elution of Eu on LN resin (third step of the protocol as shown on Figure 1). Initial loading was 1 µg of NIST 3117a.
B) Cumulated Eu isotopic composition of the combined fractions. Blue and yellow points are two different batches (i.e. two different columns). Circles show the Eu isotopic composition of the cumulated fractions from the front to the tail of the elution peak. Such trend predicts the isotopic composition of the Eu fraction if the end of the elution peak was not fully recovered. Squares show the Eu isotopic composition of the cumulated fractions from the tail to the front of the elution peak, mimicking the isotopic composition of the Eu fraction if the beginning of the elution peak has been missed.

Figure 7 Mean repeatability of Eu NIST 3117a standards

Vertical error bars correspond to the repeatability standard deviation (2SD) of each measurement sequence. The horizontal light grey band is the mean repeatability and the dark grey band is our adopted repeatability (2SD = ± 0.5 ε).

Figure 8 Eu isotopic compositions of geological reference materials

Vertical error bars correspond to 2SE. The horizontal grey band is our estimated repeatability (2SD = ± 0.5 ε).

8 References

1 I. M. Ismail, M. Nomura and Y. Fujii, *J. Chromatogr. A*, 1998, **808**, 185–191.

2 I. Ismail, M. Nomura and Y. Fujii, *J. Nucl. Sci. Technol.*, 1998, **35**, 801–807.

3 M. Bau, *Chem. Geol.*, 1991, **93**, 219–230.

4 A. Danielson, P. Möller and P. Dulski, *Chem. Geol.*, 1992, **97**, 89–100.

5 D. A. Sverjensky, *Earth Planet. Sci. Lett.*, 1984, **67**, 70–78.

6 J. Meija, T. B. Coplen, M. Berglund, W. A. Brand, P. De Bièvre, M. Gröning, N. E. Holden, J. Irrgeher, R. D. Loss, T. Walczyk and T. Prohaska, *Pure Appl. Chem.*, 2016, **88**, 293–306.

7 G. G. Arantes De Carvalho, P. V. Oliveira and L. Yang, *J. Anal. At. Spectrom.*, 2017, **32**, 987–995.

8 F. Moynier, A. Bouvier, J. Blichert-Toft, P. Telouk, D. Gasperini and F. Albarède, *Geochim. Cosmochim. Acta*, 2006, **70**, 4287–4294.

9 -G Lee and T. Tanaka, *Geochem. J.*, 2021, **55**, e9e17.

10 S. G. Lee and T. Tanaka, *Spectrochim. Acta - Part B At. Spectrosc.*, 2019, **156**, 42–50.

11 S. G. Lee and T. Tanaka, *Int. J. Mass Spectrom.*, 2021, **469**, 116668.

12 Z. Yu, P. Robinson and P. McGoldrick, *Geostand. Newsl.*, 2001, **25**, 199–217.

13 W. Zhang, Z. Hu, Y. Liu, H. Chen, S. Gao and R. M. Gaschnig, *Anal. Chem.*, 2012, **84**, 10686–10693.

14 J. Barling and D. Weis, *J. Anal. At. Spectrom.*, 2008, **23**, 1017–1025.

15 J. Barling and D. Weis, *J. Anal. At. Spectrom.*, 2012, **27**, 653–662.

16 J. W. Olesik, *Inductively Coupled Plasma Mass Spectrometers*, Elsevier Ltd., 15th edn., 2013, vol. 15.

17 C. N. Maréchal, P. Télouk and F. Albarède, *Chem. Geol.*, 1999, **156**, 251–273.

18 E. Frères, D. Weis, K. Newman, M. Amini and K. Gordon, *Geostand. Geoanalytical Res.*, 2021, **45**, 501–523.

19 F. Albarède, P. Telouk, J. Blichert-Toft, M. Boyet, A. Agranier and B. Nelson, *Geochim. Cosmochim. Acta*, 2004, **68**, 2725–2744.

20 L. Yang, *Mass Spectrom. Rev.*, 2009, **28**, 990–1011.

21 G. Audi, M. Wang, A. H. Wapstra, F. G. Kondev, M. MacCormick, X. Xu and B. Pfeiffer, *Chinese Phys. C*, 2012, **36**, 1287–1602.

22 H. Hidaka, M. Ebihara and M. Shima, *Anal. Chem.*, 1995, **67**, 1437–1441.

23 H. Hidaka, M. Ebihara and S. Yoneda, *Meteorit. Planet. Sci.*, 2000, **35**, 581–589.

24 H. Hidaka, M. Ebihara and S. Yoneda, *Earth Planet. Sci. Lett.*, 2000, **180**, 29–37.

25 H. Hidaka and S. Yoneda, *Geochim. Cosmochim. Acta*, 2007, **71**, 1074–1086.

26 M. Bavio, M. Fernández, E. Zubillaga, R. Servant and E. Gautier, *Microchem. J.*, 2016, **128**, 320–324.

27 O. Eugster, F. Tera, D. S. Burnett and G. J. Wasserburg, 1970, **7**, 436–440.

28 J. E. Sansonetti and W. C. Martin, *J. Phys. Chem. Ref. Data*, 2005, **34**, 1559–2259.

29 D. York, N. M. Evensen, M. L. Martínez and J. De Basabe Delgado, *Am. J. Phys.*, 2004, **72**, 367–375.

30 S. Wakaki and T. Tanaka, *Int. J. Mass Spectrom.*, 2012, **323–324**, 45–54.

31 N. S. Saji, D. Wielandt, C. Paton and M. Bizzarro, *J. Anal. At. Spectrom.*, 2016, **31**, 1490–1504.

32 T. Yokoyama, A. Makishima and E. Nakamura, *Chem. Geol.*, 1999, **157**, 175–187.

Table 1 Chemical protocol used for the purification of Eu using cationic and column chromatography techniques

	Reagents	Volume (mL)
AG® 50W-X8 Cation exchange resin 200-400 mesh, hydrogen form (2mL of resin) - Separate REE from major elements		
Load sample	2.5 M HCl – 0.3 M HF	2
Discard major elements	2.5 M HCl	2 * 0.75 + 2 * 5
Partially discard Ba	2 M HNO_3	2 * 4
Collect REE	6 M HCl	2 * 6.5
Eichrom™ TRU resin 50-100 mm (250 µL of resin) – Purify REE from Ba		
Load sample	1 M HNO_3	3 * 0.5
Discard Ba	1 M HNO_3	2 * 0.5 + 3
Collect REE	0.05 M HNO_3	3*3
Eichrom™ LN resin 20-50 mm (400 mg of resin) – Separate Eu from other REE		
Load sample	0.5 M HCl	0.2
Discard LREE	0.5 M HCl	4.5
Collect Eu	0.5 M HCl	3.7

Table 2 Isotopic composition of NIST 3117a processed through chemistry

Date (yyyy/mm/dd)	Eu NIST 3117a – Sm NIST 3147a concentration (ppb - ppb)	Batch/Sample	$^{153}Eu/^{151}Eu$ Raw	2SE[a]	$^{153}Eu/^{151}Eu$ corrected using $\beta Sm = A(\beta Eu) + B$	2SE	εEu	2SE	Yield (%)
NIST 3117a processed through LN resin (third step of the protocol) only									
2021/12/20	10-20	Batch 1 - NIST 1	1.108881	0.000007	1.091593	0.000013	-0.10	0.13	98
2021/12/20	10-20	Batch 1 - NIST 2	1.108912	0.000016	1.091647	0.000013	0.42	0.13	98
2021/12/20	10-20	Batch 1 - NIST 3	1.108973	0.000010	1.091633	0.000012	0.32	0.12	90
2021/12/20	10-20	Batch 1 - NIST 4	1.109307	0.000023	1.091619	0.000012	0.18	0.12	95
2021/12/20	10-20	Batch 1 - NIST 5	1.108938	0.000011	1.091616	0.000013	0.17	0.13	95
2021/12/20	10-20	Batch 1 - NIST 6	1.108790	0.000010	1.091588	0.000016	-0.13	0.16	97
2021/12/20	10-20	Batch 1 - NIST 7	1.108778	0.000010	1.091626	0.000014	0.14	0.14	95
2021/12/20	10-20	Batch 1 - NIST 8	1.108809	0.000012	1.091632	0.000017	0.25	0.17	99
2021/12/20	10-20	Batch 1 - NIST 9	1.108704	0.000011	1.091630	0.000017	0.36	0.17	95
NIST 3117a processed through all resins (full protocol)									
2022/06/23	10-20	Batch 2 - NIST 1	1.111783	0.000009	1.091648	0.000020	-0.22	0.4	97
2022/06/23	10-20	Batch 2 - NIST 2	1.111861	0.000020	1.091586	0.000018	-0.38	0.4	100
2022/06/23	10-20	Batch 2 - NIST 3	1.11184	0.000032	1.091573	0.000029	-0.51	0.4	100
2022/06/23	10-20	Batch 2 - NIST 4	1.111689	0.000027	1.091582	0.000012	-0.44	0.4	100

[a] SE stands for "standard error" and corresponds to internal error.

Table 3 Eu isotopic composition of geological reference materials

Geological reference material	Sequence date (yyyy/mm/dd)	Eu (ppm)[c]	Digestion	Yields (%)	Ba/Eu in the separated Eu fraction	ε_{Eu}	2SE[d]	2SD[e]	SiO2 (wt %)[c]
Andesite									
AGV-1	2021/10/04	1.545	HF-HNO3	92	Absence of Ba	0.26	0.12	0.27	58.6
AGV-1 (rerun[a])	2021/10/04	1.545	HF-HNO3	92	Absence of Ba	0.26	0.1	0.27	58.6
AGV-2	2021/11/11	1.545	NH4HF2	95	Absence of Ba	0.42	0.13	0.14	58.6
Anorthosite									
AN-G	2021/11/11	0.37	HF-HNO_3	79	Absence of Ba	0.40	0.12	0.14	46.3
AN-G (duplicate[b])	2022/02/16	0.37	NH_4HF_2	98	Absence of Ba	0.45	0.29	0.42	46.3
Basalt									
BCR-1	2021/11/11	1.96	HF-HNO_3	80	Absence of Ba	0.20	0.12	0.14	54.1
BHVO-2	2021/10/04	2	HF-HNO_3	100	Absence of Ba	0.11	0.11	0.27	49.5
BHVO-2 (rerun)	2021/10/04	2	HF-HNO_3	100	Absence of Ba	0.24	0.10	0.27	49.5
BHVO-2 (duplicate)	2023/01/26	2	HF-HNO_3	82	Absence of Ba	- 0.43	0.1	0.17	49.5
BHVO-2 (duplicate rerun 1)	2023/01/26	2	HF-HNO_3	82	Absence of Ba	- 0.46	0.09	0.17	49.5
BHVO-2 (duplicate rerun 2)	2023/01/27	2	HF-HNO_3	82	Absence of Ba	- 0.11	0.2	0.28	49.5
BHVO-2 (duplicate rerun 3)	2023/01/27	2	HF-HNO_3	82	Absence of Ba	- 0.15	0.16	0.28	49.5
BIR 1a	2021/10/04	0.5	HF-HNO_3	80	Absence of Ba	0.62	0.12	0.27	47.4
BIR 1a (duplicate)	2021/11/11	0.5	HF-HNO_3	85	Absence of Ba	0.50	0.29	0.14	47.4
Granite									
G-2	2021/10/04	1.4	HF-HNO_3	79	Absence of Ba	0.20	0.17	0.27	68.7
G-2 (rerun)	2021/10/04	1.4	HF-HNO_3	79	Absence of Ba	0.15	0.12	0.27	68.7
G-2 (duplicate)	2021/02/16	1.4	NH_4HF_2	100	Absence of Ba	0.38	0.24	0.42	68.7
Rhyolite									
RGM-1	2021/11/11	0.64	HF-HNO_3	81	Absence of Ba	0.19	0.10	0.14	72.6
RGM-1 (duplicate)	2022/02/16	0.64	NH_4HF_2	87	Absence of Ba	- 0.46	0.20	0.42	72.6
Terrigenous sediments									
JLk-1	2021/10/04	1.2	HF-HNO_3	87	Absence of Ba	0.35	0.12	0.27	57.7
JLk-1 (rerun)	2021/10/04	1.2	HF-HNO_3	87	Absence of Ba	0.28	0.14	0.27	57.7
JLk-1 (duplicate)	2022/02/16	1.2	NH_4HF_2	83	Absence of Ba	0.85	0.27	0.42	57.7
JSd-2	2021/10/04	0.8	HF-HNO_3	91	Absence of Ba	0.22	0.11	0.27	60.9
JSd-2 (duplicate 1)	2021/11/11	0.8	HF-HNO_3	87	Absence of Ba	- 0.35	0.1	0.14	60.9
JSd-2 (duplicate 2)	2022/02/16	0.8	NH_4HF_2	100	Absence of Ba	- 0.20	0.57	0.42	60.9

[a] "Rerun" stands for the measurement of the same sample separated in a different measurement sequence.

[b] "Duplicate" stands for a complete digestion duplicate (i.e. new digestion).

[c] Europium and SiO_2 contents reported in the table are from GeoReM website[1].

[d] "SE" stands for "standard error and corresponds to internal errors.

[e] "SD" stands for "standard deviation and is calculated using the different analyses of the same standard during a measurement sequence.

1. References

1 K. P. Jochum, U. Nohl, K. Herwig, E. Lammel, B. Stoll and A. W. Hofmann, *Geostand. Geoanalytical Res.*, 2005, **29**, 333–338.

Table 4 Neptune Plus MC-ICP-MS Instrument settings

RF Power	1200 W
Cool gas	15 $L.min^{-1}$
Auxiliary gas	0.75 – 0.85 $L.min^{-1}$
Nebulizer gas	0.9-1.0 $L.min^{-1}$
Sample cone	Jet, ø = 1.2 mm, nickel
Skimmer cone	X, ø = 0.8 mm, nickel
Introduction system	Aridus II from CETAC Technologies™
Sample uptake rate	Nebulizer 100 $\mu L.min^{-1}$
Sample uptake time	30 s
Wash time	0.7 M HNO_3 for 600 s, then 0.05 M HNO_3 for 360 s
Scan type	Static measurements
Zoom optics	Focus quad: 0 V, dispersion quad: 0 V
Sensivity	~ 0.9 V/ppb for ^{151}Eu
Integration time	8.389 s
Number of integrations	1
Block/Cycles for regular sample	1/60

Table 5 Cup configuration used to analyze Eu isotopic compositions on the Neptune Plus MC-ICP-MS

Cup	L4	L3	L2	L1	Ax	H1	H2	H3	H4
Amplifier (Ohm)	10^{11}	10^{11}	10^{11}	10^{11}	10^{11}	10^{11}	10^{11}	10^{11}	10^{10}
Mass	147	149	150	151	152	153	155	156	157
Element	Sm	Sm	Sm, Nd	Eu	Sm, Gd	Eu	Gd	Gd, Dy	Gd
Potential interferences (including oxides and hydrures)	$^{146}Nd^{1}H^{+}$	$^{148}Nd^{1}H^{+}$	$^{134}Ba^{16}O^{+}$, $^{149}Sm^{1}H^{+}$	$^{135}Ba^{16}O^{+}$, 150Sm1H^{+}	$^{136}Ba^{16}O^{+}$, $^{136}Ce^{16}O^{+}$, $^{151}Eu^{1}H^{+}$	$^{137}Ba^{16}O^{+}$, $^{152}Sm^{1}H^{+}$	$^{139}La^{16}O^{+}$	$^{140}Ce^{16}O^{+}$, $^{155}Gd^{1}H^{+}$	$^{141}Pr^{16}O^{+}$, $^{156}Gd^{1}H^{+}$

Table 6 Average Eu isotopic compositions of NIST 3117a standards

Sequence date (dd/mm/yyyy)	NIST 3117a Eu – NIST 3147a Sm concentration (ppb - ppb)	Standard[a] or Sample-Standard[b] measurement	$^{153}Eu/^{151}Eu$ Raw	2SD[d]	n[e]	$^{153}Eu/^{151}Eu$ corrected with β_{Sm}	2SD	Slope A $\beta Sm = A(\beta Eu) + B$[c]	Intercept B $\beta Sm = A(\beta Eu) + B$[c]	$^{153}Eu/^{151}Eu$ corrected with $\beta Sm = A(\beta Eu) + B$	2SD	εEu calculated with $\beta Sm = A(\beta Eu) + B$	2SD
2021/02/16	10-24	Standard	1.106761	0.000430	8	1.094857	0.000022	0.9581	0.1821	1.091602	0.000016	0.00	0.18
2021/02/16	14-32	Standard	1.106699	0.000215	8	1.094929	0.000015	0.9854	0.2158	1.091602	0.000014	0.01	0.22
2021/03/03	10-24	Standard	1.106539	0.000505	8	1.094868	0.000020	1.0185	0.2457	1.091604	0.000018	-0.01	0.15
2021/03/03	14-32	Standard	1.106585	0.000225	8	1.094954	0.000012	0.9828	0.2151	1.091600	0.000012	0.00	0.21
2021/06/28	14-32	Standard	1.110225	0.000120	6	1.094916	0.000008	1.0388	0.2801	1.091599	0.000007	0.00	0.12
2021/10/04	20-40	Standard	1.106017	0.000417	7	1.094840	0.000032	0.9667	0.1931	1.091581	0.000026	-0.01	0.21
2021/10/04	20-40	Sample-Standard	1.105093	0.000307	16	1.094827	0.000022	0.9499	0.1751	1.091634	0.000025	-0.01	0.27
2021/11/08	20-40	Standard	1.107730	0.000328	7	1.094913	0.000024	0.9568	0.1818	1.091602	0.000022	0.00	0.24
2021/11/09	20-40	Standard	1.107194	0.000503	7	1.094861	0.000028	0.9641	0.1879	1.091599	0.000017	0.00	0.18
2021/11/09	20-40	Sample-Standard	1.106270	0.000132	12	1.094858	0.000038	1.2099	0.4386	1.091604	0.000018	-0.01	0.15
2021/11/10	15-30	Standard	1.107746	0.000289	5	1.094884	0.000028	0.9594	0.1828	1.091599	0.000025	-0.01	0.29
2021/11/10	15-30	Sample-Standard	1.107155	0.000548	12	1.094868	0.000015	0.9914	0.2177	1.091600	0.000015	0.01	0.21
2021/12/15	20-40	Standard	1.109583	0.000453	6	1.094913	0.000029	0.9443	0.1611	1.091598	0.000029	0.01	0.46
2021/12/16	10-20	Standard	1.111061	0.002801	27	1.095011	0.000107	0.9662	0.1917	1.091597	0.000055	0.01	0.38
2021/12/17	10-20	Standard	1.109108	0.000744	27	1.094962	0.000037	0.9458	0.1686	1.091590	0.000027	0.00	0.22
2021/12/20	10-20	Standard	1.109024	0.000459	7	1.094893	0.000016	1.0028	0.2322	1.091598	0.000016	-0.01	0.25
2021/12/20	10-20	Sample-Standard	1.108770	0.000254	13	1.094900	0.000022	1.0605	0.3008	1.091600	0.000015	0.01	0.19
2021/12/21	10-20	Standard	1.109117	0.000137	7	1.094918	0.000036	0.9248	0.1394	1.091602	0.000037	0.04	0.49
2021/12/21	10-20	Sample-Standard	1.109033	0.000210	12	1.094913	0.000025	0.8918	0.0998	1.091601	0.000016	-0.01	0.24
2022/02/14	10-20	Standard	1.108659	0.000530	7	1.094920	0.000041	0.9702	0.1954	1.091601	0.000029	0.05	0.47

2022/02/14	10-20	Sample-Standard	1.106591	0.000265	14	1.094962	0.000046	0.9748	0.2074	1.091599	0.000046	0.00	0.51
2022/02/15	10-20	Standard	1.106952	0.000352	7	1.094900	0.000038	0.9342	0.1596	1.091597	0.000035	0.05	0.65
2022/02/15	10-20	Sample-Standard	1.106439	0.000246	8	1.094911	0.000028	1.0380	0.2688	1.091600	0.000027	-0.02	0.32
2022/02/16	10-20	Standard	1.107336	0.000805	7	1.094923	0.000047	0.9453	0.1713	1.091600	0.000017	-0.02	0.19
2022/02/16	10-20	Sample-Standard	1.106396	0.000688	13	1.094911	0.000040	1.0098	0.2397	1.091603	0.000043	-0.04	0.42
2022/04/20	10-20	Standard	1.109165	0.000788	7	1.095030	0.000026	0.9876	0.2231	1.091600	0.000023	0.01	0.34
Mean						**1.094909**	**0.000031**	**0.9838**	**0.2106**	**1.091600**	**0.000024**	**0.00**	**0.29**

[a] "Standard sequences" correspond to measurement sequences during which we only measured NIST 3117a standards. Such sequences usually precede "Sample-Standard sequences". "Standard sequences" are useful to check the stability of the instrument and the repeatability of the measurements before analyses. Between those sequences, we sometimes needed to slightly adjust the gas rate without modifying the torch parameters in order to get the most sensitive signal.

[b] "Sample-Standard sequences" correspond to measurement sequences during which we measured samples and standards.

[c] We treat these two sequences independently to determine the regression slopes and intercepts between β_{Sm} and β_{Eu} even if the two sequences were performed the same day. "Slope A" and "Intercept B" are the slope and intercept of the weighted linear regression between β_{Sm} and β_{Eu} for each sequence.

[d] "SD" stands for standard deviation.

[e] "n" is the number of NIST 3117a standards measured in each sequence.

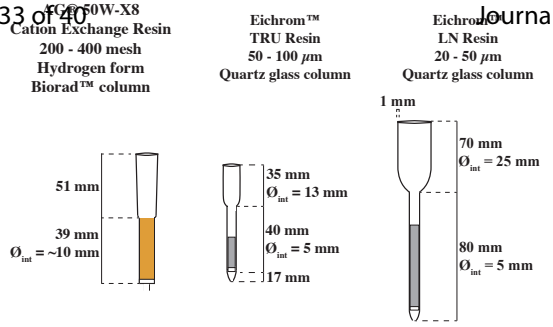
AG® 50W-X8
Cation Exchange Resin
200 - 400 mesh
Hydrogen form
Biorad™ column
Eichrom™
TRU Resin
50 - 100 μm
Quartz glass column
Eichrom™
LN Resin
20 - 50 μm
Quartz glass column
51 mm
39 mm
Ø int = ~10 mm
35 mm
Ø int = 13 mm
40 mm
Ø int = 5 mm
17 mm
1 mm
70 mm
Ø int = 25 mm
80 mm
Ø int = 5 mm

B

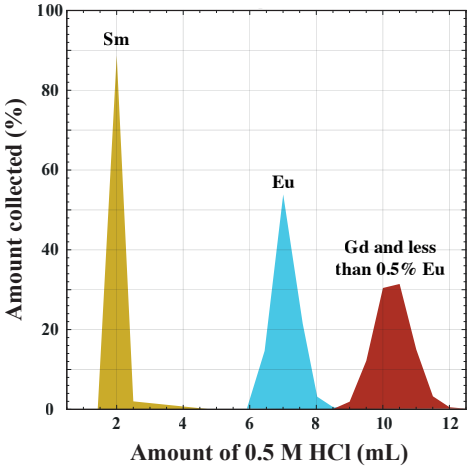
Sm
Eu
Gd and less
than 0.5% Eu
Amount collected (%)
Amount of 0.5 M HCl (mL)
0
20
40
60
80
100
2
4
6
8
10
12

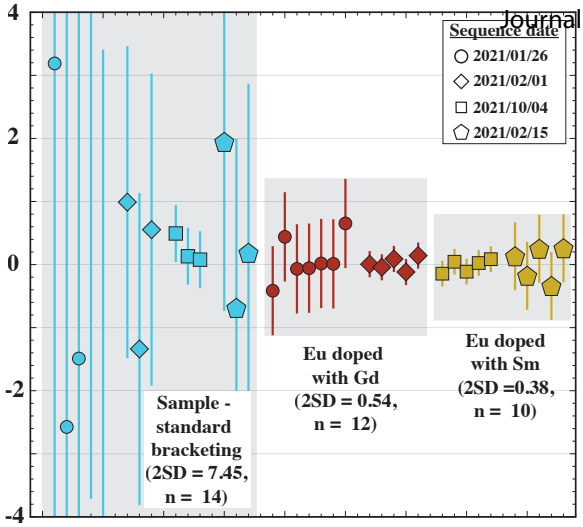
Sequence date
2021/01/26
2021/02/01
2021/10/04
2021/02/15
δ Eu
4
2
0
-2
-4
Sample - standard bracketing (2SD = 7.45, n = 14)
Eu doped with Gd (2SD = 0.54, n = 12)
Eu doped with Sm (2SD =0.38, n = 10)

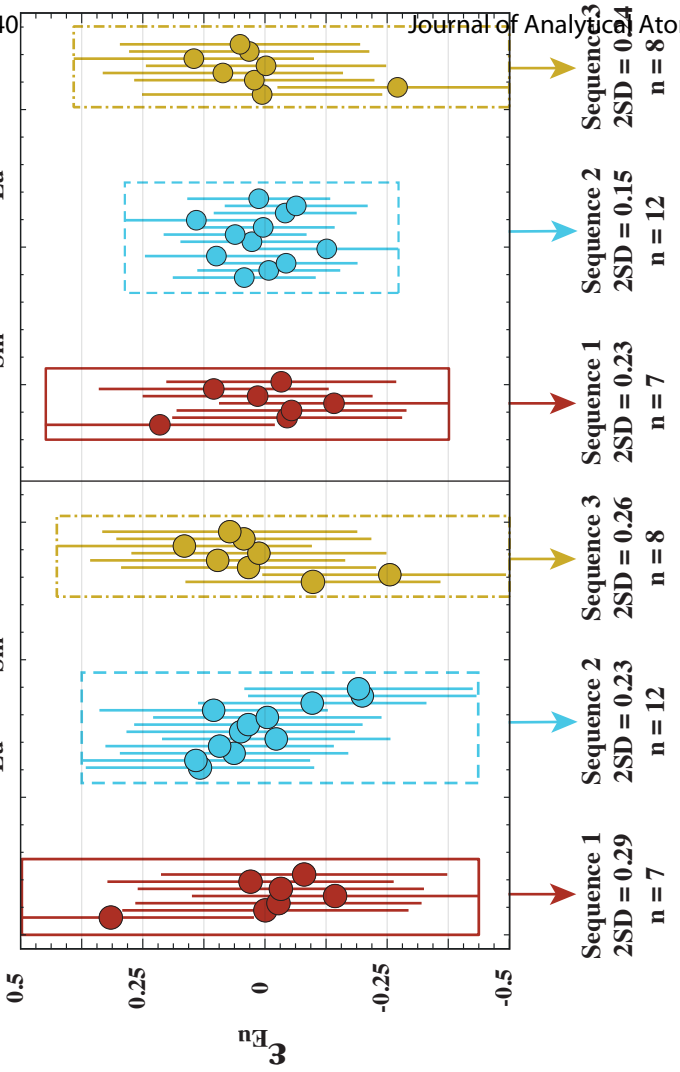
βSm = a * βEu + b
βEu = βSm
εEu
0.5
0.25
0
-0.25
-0.5
Sequence 1
2SD = 0.29
n = 7
Sequence 2
2SD = 0.23
n = 12
Sequence 3
2SD = 0.26
n = 8
Sequence 1
2SD = 0.23
n = 7
Sequence 2
2SD = 0.15
n = 12
Sequence 3
2SD = 0.24
n = 8

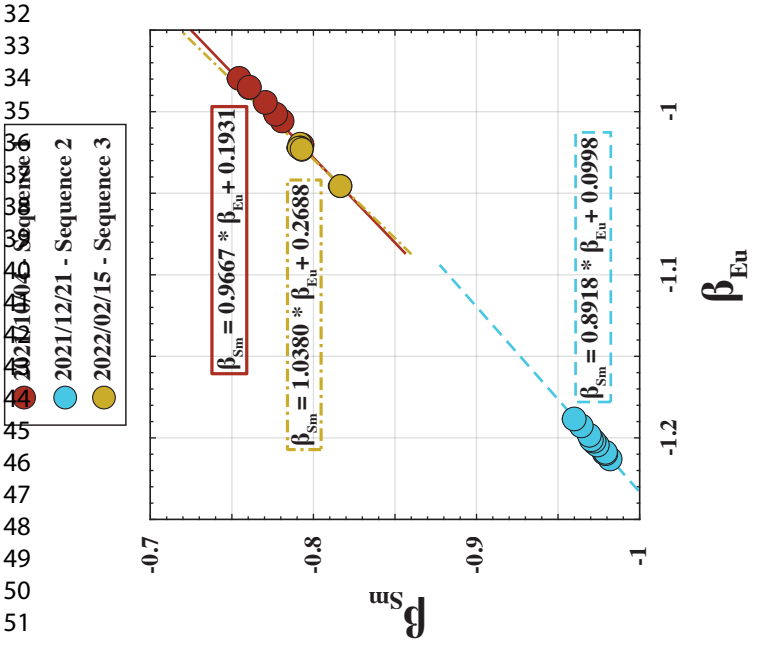
2021/12/21 - Sequence 2
2022/02/15 - Sequence 3
βSm = 0.9667 * βEu + 0.1931
βSm = 1.0380 * βEu + 0.2688
βSm = 0.8918 * βEu + 0.0998
βSm
βEu
-0.7
-0.8
-0.9
-1
-1
-1.1
-1.2

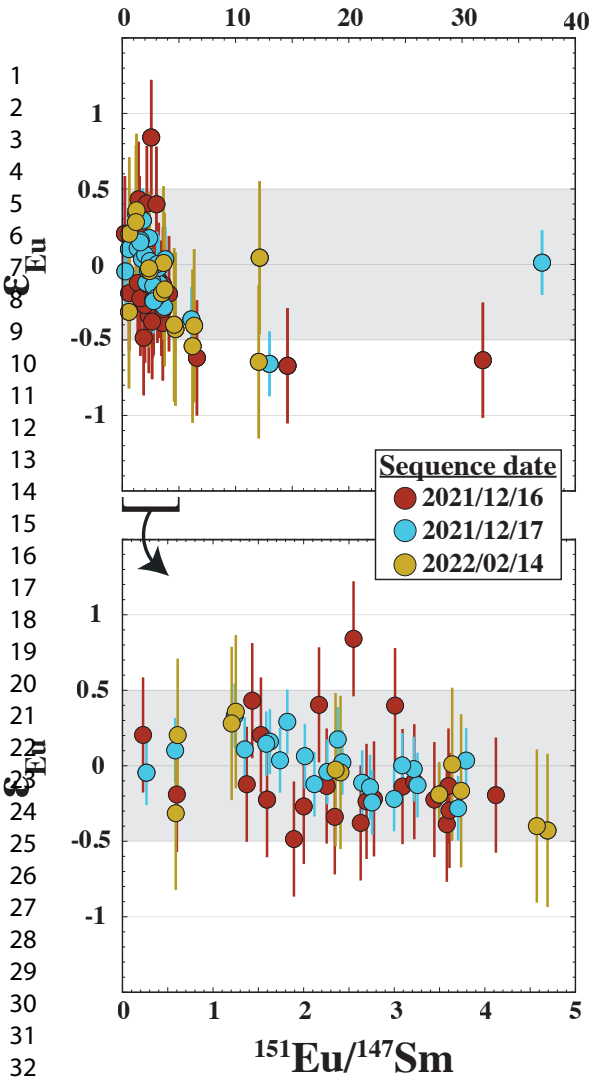
0
10
20
30
40
1
0.5
0
-0.5
-1
ε_{Eu}
Sequence date
2021/12/16
2021/12/17
2022/02/14
0
1
2
3
4
5
$^{151}Eu/^{147}Sm$

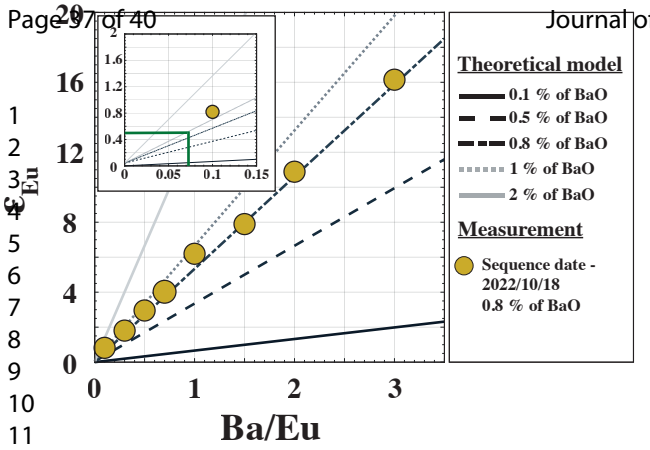
20
16
12
8
4
0
0
1
2
3
Ba/Eu
Theoretical model
0.1 % of BaO
0.5 % of BaO
0.8 % of BaO
1 % of BaO
2 % of BaO
Measurement
Sequence date -
2022/10/18
0.8 % of BaO
2
1.6
1.2
0.8
0.4
0
0
0.05
0.1
0.15

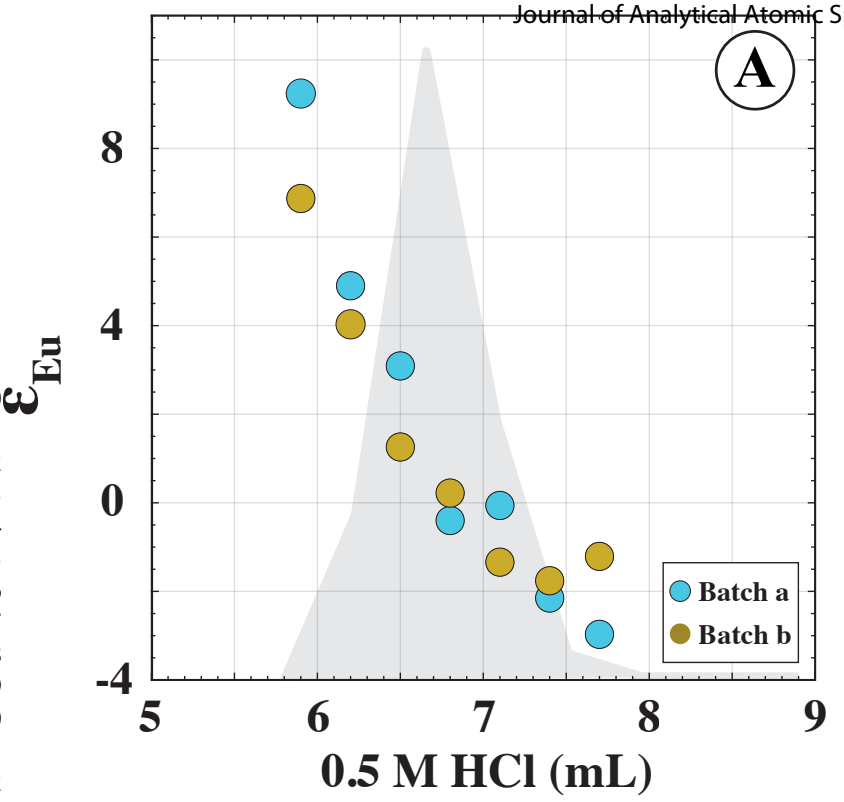
A
8
4
0
-4
5
6
7
8
9
ε_{Eu}
0.5 M HCl (mL)
Batch a
Batch b

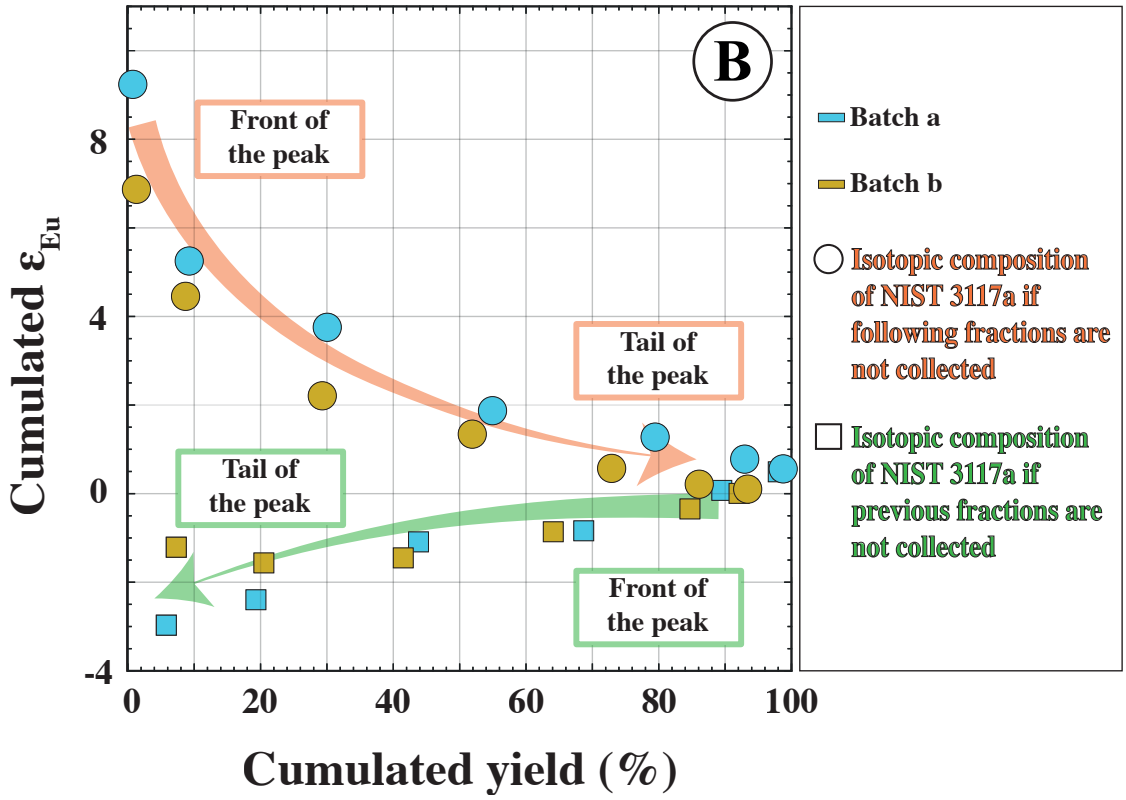
B
Front of the peak
Tail of the peak
Tail of the peak
Front of the peak
8
4
0
-4
0
20
40
60
80
100
Cumulated ε_{Eu}
Cumulated yield (%)
Batch a
Batch b
Isotopic composition of NIST 3117a if following fractions are not collected
Isotopic composition of NIST 3117a if previous fractions are not collected

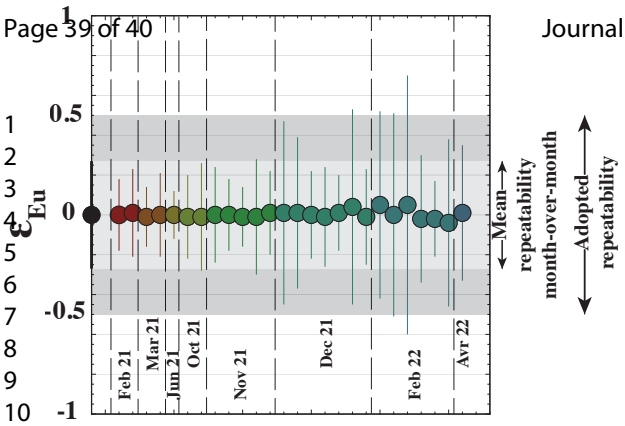
1
0.5
0
-0.5
-1
ε_{Eu}
Feb 21
Mar 21
Jun 21
Oct 21
Nov 21
Dec 21
Feb 22
Avr 22
Mean repeatability month-over-month
Adopted repeatability

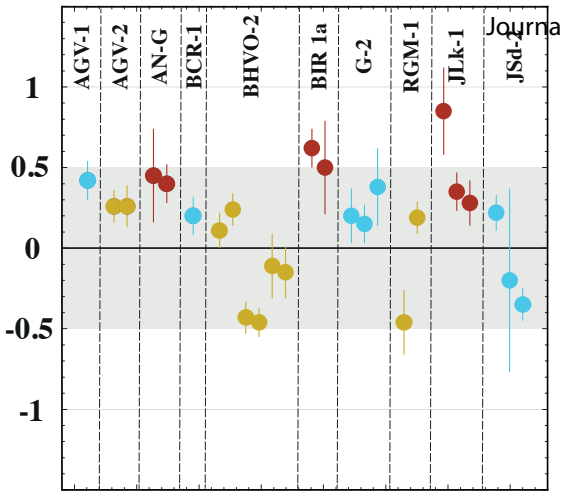
AGV-1
AGV-2
AN-G
BCR-1
BHVO-2
BIR 1a
G-2
RGM-1
JLk-1
JSd-2
1
0.5
0
-0.5
-1
ε_{Eu}